

Anharmonic mixing between two phonons in red mercury iodide

A. Anedda and G. Bongiovanni*

Dipartimento di Scienze Fisiche, Università degli Studi di Cagliari, via Ospedale 72, I-09100 Cagliari, Italy

(Received 23 June 1988)

With use of Raman spectroscopy we have investigated the anharmonic mixing between two optical phonons of E_g symmetry in red mercury iodide. By taking into account the presence of several decay channels contributing to phonon lifetime, the experimental line-shape anomalies due to mode coupling have been reproduced with good accuracy. The temperature behavior of the anharmonic interaction is in agreement with theory.

I. INTRODUCTION

First-order Raman light scattering is a powerful tool for investigating optical phonons whose wave vector is close to the center of the Brillouin zone. With the aid of group theory it is possible to analyze experimental spectra and obtain typical crystal parameters related to interactions among atoms in the lattice. Resonance linewidth is mainly the consequence of the finite lifetime of the normal modes interacting with a continuum of two or more phonons. This coupling is introduced by anharmonic terms in the atomic displacement expansion of crystal total energy. Broadening is indeed the immediate evidence of this interaction; however, the study of finer details, such as line-shape anomalies,¹⁻³ is important in order to have a more complete knowledge of the microscopic phonon coupling in crystals.

In addition to line broadening, the interaction of a one-phonon state with the continuum, for example, of two phonons gives an interference effect well described by Fano's theory.¹⁻⁴ Nevertheless, it requires that two-phonon states are Raman active, a process which is

known to be of second order. We can also have an interference effect between two Raman modes $|\phi_1\rangle$ and $|\phi_2\rangle$ with the same symmetry,^{1,5} when anharmonicity couples the two optical vibrations. The resulting line-shape distortion can be explained as due to interference from the Raman amplitude of the one-step transition $\langle \phi_{1(2)} | R_{1(2)} | \phi_0 \rangle$ with the three-step transition

$$\langle \phi_{1(2)} | H_{\text{anh}} | \phi_c \rangle \langle \phi_c | H_{\text{anh}} | \phi_{2(1)} \rangle \langle \phi_{2(1)} | R_{2(1)} | \phi_0 \rangle$$

(see Fig. 1). In both cases only the phonon $|\phi_{1(2)}\rangle$ is created, but while the first process is the usual one, the second is indirect. It requires the presence of the Raman-active phonon $|\phi_{2(1)}\rangle$ and the multiphonon states $|\phi_c\rangle$, coupled to modes $|\phi_1\rangle$ and $|\phi_2\rangle$ by the anharmonic Hamiltonian H_{anh} . Anyway, mixing between two optical phonons is not always possible; for example, it is forbidden for diatomic crystals with NaCl structure by symmetry considerations.⁶ In fact, crystal symmetry, the detailed structures of the continuum states $|\phi_c\rangle$, and temperature play an essential role in the phonon line shape.

Our aim is to investigate their influence on the anharmonic mixing between two phonons of E_g symmetry in mercury iodide.^{7,8} For this compound a reasonable interpretation of Raman spectra has been given quite recently⁹⁻¹² and the study of anharmonicity is still an open problem.^{7,9,13} The E_g phonons are particularly suitable for studying mode interaction and its behavior with temperature because (1) they have a good Raman efficiency when excited with photon energy close to the band gap (this allows us to perform a reliable line-shape analysis), and (2) the crystal anisotropy lifts the degeneracy of the acoustic bands, making it possible to investigate how the presence of several decay (scattering) channels affects phonon line shape.

In the first part of this paper we develop a model which accounts for two-phonon mixing at temperatures different from 0 K. Then a comparison with the previous models is presented. In the second part an analysis of the experimental data with our model is performed.

II. SPECTRAL SHAPE OF TWO MODES COUPLED INDIRECTLY BY ANHARMONIC FORCES

The Raman spectral shape of two optical phonons is related to the phonon correlation functions $\Phi_{i,j}$ as follows:⁵

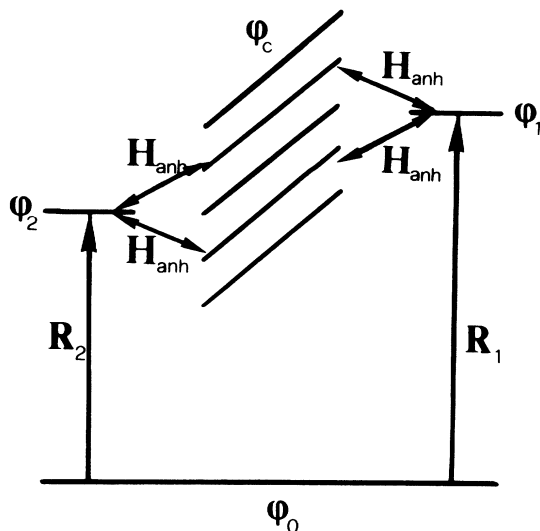


FIG. 1. Schematic representation of Raman scattering by two phonons coupled indirectly by the perturbation Hamiltonian H_{anh} . The ground state $|\phi_0\rangle$ is connected to the phonon state $|\phi_1\rangle$ ($|\phi_2\rangle$) both directly and indirectly, via the state $|\phi_2\rangle$ ($|\phi_1\rangle$) and the continuum of two acoustic-phonon states $|\phi_c\rangle$.

$$R(\mathbf{k}, \omega, T) = \sum_{i,j} \int dt \int dt' \int dx \int dx' A_i A_j e^{i[\omega(t-t') - \mathbf{k}(\mathbf{x}-\mathbf{x}')] } \langle \phi_i(\mathbf{x}, t) \phi_j(\mathbf{x}', t') \rangle \\ \times \sum_{i,j} \int dt \int dt' \int dx \int dx' A_i A_j e^{i[\omega(t-t') - \mathbf{k}(\mathbf{x}-\mathbf{x}')] } \Phi_{i,j}, \quad (1)$$

where $\phi_i(\mathbf{x}, t)$ is the phonon-field operator associated with the i th-optical mode, A_i^2 is its Raman strength, and $\langle \rangle$ represents the canonical ensemble average; k must be taken $\simeq 0$ due to the small value of the wave vector of the photon involved in Raman scattering.

In order to find an explicit form of Eq. (1), we introduce the temperature Green's functions defined as¹⁴

$$D_{i,j} \equiv \langle T_\tau [\phi_i(\mathbf{x}', \tau') \phi_j(\mathbf{x}, \tau)] \rangle, \quad (2)$$

with $\phi_i(\mathbf{x}, \tau) \equiv e^{H\tau} \phi_i e^{-H\tau}$ and T_τ the time- τ ordering operator. Then the phonon propagator $D_{i,j}(\mathbf{k}, \omega_l)$ is defined as the Fourier coefficient of $D_{i,j}$,¹⁵ where ω_l are the Matsubara frequencies for a boson field.

The relation between the Fourier transform of the true time correlation function $\Phi_{i,j}$ and $D_{i,j}(\mathbf{k}, i\omega_l \rightarrow \omega)$ is given by¹⁵

$$\lim_{\epsilon \rightarrow 0^+} \frac{D_{i,j}(\mathbf{k}, \omega + i\epsilon) - D_{i,j}(\mathbf{k}, \omega - i\epsilon)}{2\pi i} = \frac{1}{2\pi\beta\hbar} (1 - e^{-\beta\hbar\omega}) \Phi_{i,j}(\mathbf{k}, \omega), \quad (3)$$

with $\beta = k_B T$. From the last equation we can see that all we need is the propagator $D_{i,j}$. The unperturbed free-phonon propagator $D_{i,j}^0$ is

$$D_{i,j}^0 = \delta_{i,j} \frac{2\omega(\mathbf{k}, j)}{\beta\hbar} \frac{1}{\omega_l^2 + \omega^2(\mathbf{k}, j)}, \quad (4)$$

where $\omega(\mathbf{k}, i)$ is the frequency of the mode with wave vector \mathbf{k} of the i th-phonon branch. The relation between $D_{i,j}^0$ and $D_{i,j}$ is given by the Dyson equation, which becomes, in matrix notation,

$$\mathbf{D} = \mathbf{D}^0 + \mathbf{D}^0 \mathbf{G} \mathbf{D}, \quad (5)$$

where $G_{i,j}$ is the phonon proper self-energy. When only two modes are involved the $D_{i,j}$ elements are easily found by inversion of Eq. (5):

$$D_{i,j} = \frac{\delta_{i,j} D_i^0 + (-1)^{i+j+1} D_1^0 D_2^0 G_{3-j,3-i}}{1 - D_1^0 G_{1,1} - D_2^0 G_{2,2} + D_1^0 D_2^0 (G_{1,1} G_{2,2} - G_{1,2} G_{2,1})}. \quad (6)$$

At temperatures where only cubic anharmonicity is relevant, the real and imaginary parts of $G_{i,j}$, $\Delta_{i,j}$ and $\Gamma_{i,j}$, for a phonon with $k \simeq 0$, can be written as^{6,16}

$$\Delta_{i,j}(\mathbf{0}, \omega, T) = \frac{18}{\hbar^2} \sum_{\mathbf{k}_1, j_1, j_2} \frac{V(\mathbf{0}, i; \mathbf{k}_1, j_1; -\mathbf{k}_1, j_2) V(\mathbf{0}, j; -\mathbf{k}_1, j_1; \mathbf{k}_1, j_2)}{\omega(\mathbf{k}_1, j_1) \omega(\mathbf{k}_1, j_2)} \\ \times \left[\frac{(n_1 + n_2 + 1)}{[\omega - \omega(\mathbf{k}_1, j_1) - \omega(\mathbf{k}_1, j_2)]_P} - \frac{n_1 - n_2}{[\omega - \omega(\mathbf{k}_1, j_1) + \omega(\mathbf{k}_1, j_2)]_P} + \frac{n_1 - n_2}{[\omega + \omega(\mathbf{k}_1, j_1) - \omega(\mathbf{k}_1, j_2)]_P} \right], \quad (7)$$

$$\Gamma_{i,j}(\mathbf{0}, \omega, T) = \frac{18\pi}{\hbar^2} \sum_{\mathbf{k}_1, j_1, j_2} \frac{V(\mathbf{0}, i; \mathbf{k}_1, j_1; -\mathbf{k}_1, j_2) V(\mathbf{0}, j; -\mathbf{k}_1, j_1; \mathbf{k}_1, j_2)}{\omega(\mathbf{k}_1, j_1) \omega(\mathbf{k}_1, j_2)} \\ \times [(n_1 + n_2 + 1) \delta(\omega - \omega(\mathbf{k}_1, j_1) - \omega(\mathbf{k}_1, j_2)) - (n_1 - n_2) \delta(\omega - \omega(\mathbf{k}_1, j_1) + \omega(\mathbf{k}_1, j_2)) \\ + (n_1 - n_2) \delta(\omega + \omega(\mathbf{k}_1, j_1) - \omega(\mathbf{k}_1, j_2))], \quad (8)$$

where V 's are the Fourier coefficients of atomic force constants,^{6,16,17} n the thermal population factor, and $()_P$ means that the principal part must be taken. The diagonal terms $\Delta_{i,i}$ and $\Gamma_{i,i}$ are the energy shift and the line broadening of the i -phonon state. The first term of these equations corresponds to a decay of the $\omega(\mathbf{0}, i)$ phonon into two vibrations of lower energy, $\omega(\mathbf{k}_1, j_1)$ and $\omega(-\mathbf{k}_1, j_2)$. Second and third terms describe, instead, a scattering event in which the thermal phonons $\omega(\mathbf{k}_1, j_1)$ and $\omega(-\mathbf{k}_1, j_2)$ are one incoming and the other outgoing (or vice versa). The last two processes are relevant only at high temperature. If in the anharmonic processes the two-phonon states are acoustic, the real factor

$$U(i; j; j_1; j_2) \equiv \frac{V(\mathbf{0}, i; \mathbf{k}_1, j_1; -\mathbf{k}_1, j_2) V(\mathbf{0}, j; -\mathbf{k}_1, j_1; \mathbf{k}_1, j_2)}{\omega(\mathbf{k}_1, j_1) \omega(\mathbf{k}_1, j_2)} \quad (9)$$

can be approximated as \mathbf{k}_1 independent¹⁶ in the long-wavelength limit. $\Delta_{i,j}$ and $\Gamma_{i,j}$ assume the useful forms

$$\begin{aligned}\Delta_{i,j} &= \sum_{j_1, j_2} U(i; j; j_1; j_2) P(\omega; j_1; j_2; T), \\ \Gamma_{i,j} &= \sum_{j_1, j_2} U(i; j; j_1; j_2) D(\omega; j_1; j_2; T).\end{aligned}\quad (10)$$

At high temperature the function $D(\omega; j; j_2; T)$ is proportional to the density of states of the two acoustic-phonon states j_1 and j_2 times T/ω and thus it is a linear function of ωT .

Finally, combining Eqs. (1) and (3) we find that Raman Stokes cross section is given by

$$R = \beta \mathcal{N} [n(\omega) + 1] \left[\text{Im} \sum_{i,j} A_i A_j D_{i,j}(k \simeq 0, \omega) \right], \quad (11)$$

where $\text{Im}(\cdot)$ means that the imaginary part is taken.

In an ideal harmonic crystal, because of normal-mode independence no mixing among phonons exists, so that only the diagonal parts $D_{i,j} A_i^2$ are present. However, with anharmonic coupling, the off-diagonal terms in Eq. (11) contribute to Raman cross section by mixing phonons close in energy, as pointed out in the Introduction.

In order to reproduce experimental spectra, two models corresponding to different approximations of Eq. (11), are normally used. One of them, the simplest, considers two Lorentzian-like resonances and implies, as a consequence, no coupling (L model). The second one, developed solely for $T=0$ K by Zawadowski and Ruvalds (ZR model),⁵ accounts for interactions between the optical phonons in a simplified manner, i.e., a single decay channel is considered. In this case it is possible to show with little algebra⁵ that the Raman cross section vanishes at the frequency¹⁸

$$\omega_0 = \left[\frac{U_1 A_1 \omega_2 + U_2 A_2 \omega_1}{\omega_1 \omega_2 \frac{U_1 A_1 \omega_1 + U_2 A_2 \omega_2}{\omega_1 \omega_2}} \right]^{1/2}, \quad (12)$$

which lies between the phonon frequencies ω_1 and ω_2 . Moreover, only two anharmonic force constants, which couple the two optical modes with the single acoustic branch, are present. These two quantities are real and determine both linewidths and mode mixing. These constants are related directly to linewidths, so that the off-diagonal terms of the proper self-energy $G_{1,2}$ are completely fixed by the broadening values.

On the contrary, if we consider three acoustic branches whose coupling with the two optical modes is different, more than two independent parameters describing anharmonic interaction are present. If the coupling constants of optical modes with the transverse- and longitudinal-acoustic phonons are not the same, the corresponding decay channels do not interfere destructively at the same frequency, as seen from Eq. (12). This holds particularly for anisotropic crystals or crystals having many atoms in the unit cell, for which several anharmonic processes are possible for the optical modes. Thus the values of the mode-mixing parameter $G_{1,2}$ and then $\Gamma_{1,2}$ can not be fixed *a priori*. In a more realistic model $\Gamma_{1,2}$ should range between $\Gamma_{1,2} = (\Gamma_{1,1} G_{2,2})^{1/2}$ and $\Gamma_{1,2} = 0$ cm^{-1} , respec-

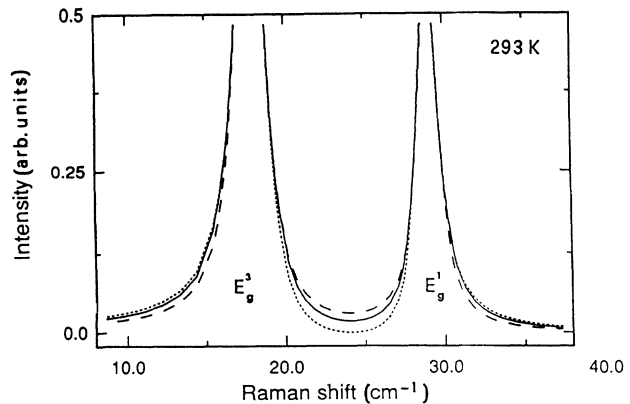


FIG. 2. Raman spectra of two optical phonons obtained with the L (---) model, the ZR ($\cdot \cdot \cdot$) model, and our model (—).

tively, for a complete interference effect⁵ or for the pure Lorentzian case. In Fig. 2 we report the theoretical curves corresponding to the L model, and ZR model, and our model at 300 K. The parameters used are typical of the E_g^2 and E_g^1 phonons as we will see later. While no difference exists among models for energy close to the peaks, the low- and high-energy sides of the resonances are distorted. The repulsive effect, caused by indirect coupling, is overestimated by ZR theory while it is completely neglected in the L case. In our model, instead, the Raman intensity can range from the two extreme approximations, depending on the relative strength of each decay channel and thus on the $G_{i,j}$ value.

III. EXPERIMENTAL RESULTS AND DISCUSSION

Mercury iodide single crystals were grown at room temperature by evaporation of proper solvent in which high-purity HgI_2 was dissolved. This “old and slow” technique gave the best results in order to have single crystals almost free from crystalline defects and thermal residual stresses.

Raman spectra were excited by a 100-mW He-Ne laser (632.8 nm). Scattered light dispersed through a 1-m Spex Industries double monochromator was detected by a cooled ITT FW130 photomultiplier. The usual photon-counting technique was used to process the signal. For variable-temperature measurements, samples were mounted strain free onto the cold finger of a closed-cycle system. The permanence of the crystal in vacuum was limited with the aim of minimizing sample damage. Incoming and outgoing photons were directed along and perpendicularly to the crystal c axis, respectively; orthogonal polarizations, one of which directed along the c axis, were used to excite E_g modes.⁹ The right-angle geometry was the best experimental configuration to reduce at very low level the diffused laser light into the spectrometer and, at the same time, to select the proper E_g polarizations. We obtained spectra virtually free from stray light and “ghosts” up to 9 cm^{-1} with a maximum resolution of

0.5 cm^{-1} . Instrumental band-pass shape was determined recording the laser line.

The crystalline structure of red mercury iodide belongs to the D_{4h}^{15} ($P4_2/nmc$) space group. It is a layered compound with six atoms per unit cell. At 25 K four Raman lines at 20, 32, 114, 143 cm^{-1} are present. The two resonances at low frequency correspond to phonons with E_g symmetry, while the 114- and 143-cm^{-1} lines are attributed to A_{1g} and B_{1g}^1 modes.⁷ The other vibrations, B_{1g}^2 and E_g^2 modes, occur at about 29 and 114 cm^{-1} (at room temperature) and are characterized by very low Raman cross section.^{9,11}

In Fig. 3 the Raman spectra of red mercury iodide are reported for four different temperatures. The energy separation of E_g resonances is about 10 cm^{-1} . At low temperature (less than 150 K) the two peaks are well separated. When temperature is raised, peaks broaden and shift towards lower frequency while their tails start to overlap. However, no zero intensity is present in the spectra between the two modes.

In order to analyze the different contributions to E_g -phonon lifetime, the phonon linewidth Γ and the energy shift Δ as a function of temperature are reported in Fig.

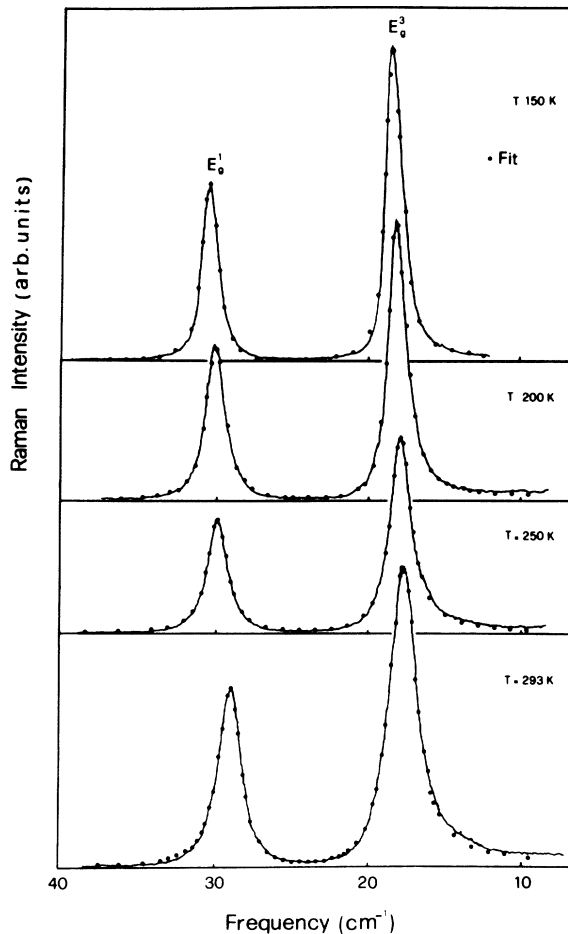


FIG. 3. Raman spectra (solid curves) of E_g^1 and E_g^3 phonons for four temperatures. Solid circles are the best fitting of experimental data.

4. A linear behavior of $\Delta_{i,i}$ and $\Gamma_{i,i}$ for both modes is displayed. The values of $d\Delta_{i,i}/dT$, $d\Gamma_{i,i}/dT$, and the linewidth at 0 K are, respectively, $d\Delta_{1,1}/dT = -7 \times 10^{-3} \text{ cm}^{-1}/\text{K}$, $d\Delta_{2,2}/dT = -9 \times 10^{-3} \text{ cm}^{-1}/\text{K}$; $d\Gamma_{1,1}/dT = 6 \times 10^{-3} \text{ cm}^{-1}/\text{K}$, $d\Gamma_{2,2}/dT = 5 \times 10^{-3} \text{ cm}^{-1}/\text{K}$; and $\Gamma_{1,1} \approx 0.0 \text{ cm}^{-1}$, $\Gamma_{2,2} \approx 0.2 \text{ cm}^{-1}$. While the linewidth variation and energy shift are in good agreement with those given by Ref. 7, we found lower values for the residual linewidths at 0 K, confirming the good quality of our samples. In the high-temperature limit the cubic term of anharmonicity gives a linear temperature dependence of linewidth and energy shift, as easily seen from Eqs. (7) and (8). Higher orders in Hamiltonian expansion give, instead, a power dependence greater than 1.¹⁹ This suggests that decay or scattering processes with three phonons are predominant for E_g modes. In addition, since for anharmonic interactions $\Gamma_{i,i} \approx \text{const} \times [n(\omega/2) + 1]$ we find, at $T=0 \text{ K}$, $\Gamma_{i,i} \approx 0 \text{ cm}^{-1}$. Therefore, according to experimental data, different broadening channels, which are independent from temperature (electron-phonon interaction, impurities, or structural defects) do not play a significant part in the E_g^3 and E_g^1 (less than 0.2 cm^{-1}) linewidths. Raman cross sections of low-frequency E_g phonons have been calculated using Eq. (11). The double degeneracy of the E_g modes strongly complicates the expression of this equation, without, however, modifying the phonon line shape significantly. By a convolution of instrumental bandpass function, the curves shown in Fig. 3 by solid circles have been obtained. Each curve represents the best fitting of the experimental data at 150, 200, 250, and 293 K. A comparison with the line shapes (solid line in Fig. 3) allows us to verify the goodness of the present model over a wide range of temperatures. At temperatures lower than 150 K, experimental spectra are still well described, but the signal-to-noise ratio makes the comparison with the

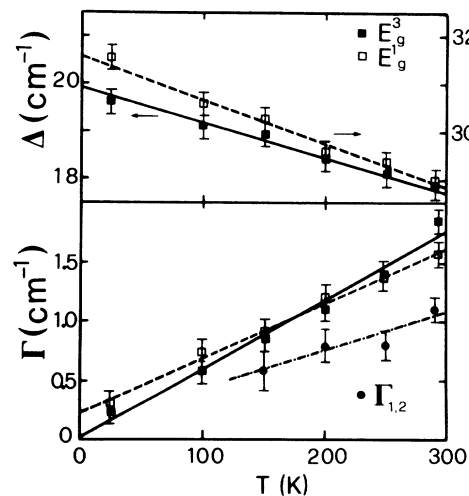


FIG. 4. Linewidth and energy shift of E_g^1 (empty squares) and E_g^3 (solid squares) vs temperature. In the lower part of the figure the mode-mixing parameter $\Gamma_{1,2} = 2\Gamma_{1,2}$ (solid squares) is reported.

theory ineffective. It is to be noted that the fitting parameters (except $\Gamma_{1,2}$) have the immediate physical meaning of intensity, broadening, and energy shift of the phonon resonances (see Fig. 4).

The energy dependence of the self-energy $G_{i,j}$ has been taken to be linear. This is a good approximation for $\Gamma_{i,j}$ as discussed in the preceding section. However, even if it does not represent the correct frequency dependence for the real part, the frequency shift $\Delta_{i,j}$ has negligible influence on the line shape. Consequently, the values of $\Delta_{1,2} = \Delta_{2,1}$ have been taken to be equal to the diagonal-part values. In the E_g^1 free-phonon propagator a constant imaginary part has been added to the real frequency. In this way we take into account perturbation effects which do not derive from anharmonicity, as suggested from the analysis of mode linewidth. It is worthwhile to remember that the use of a convolution technique rules out the influence of the instrumental finite resolution as the cause of nonzero Raman scattering at ω_0 . At room temperature the value obtained for $2\Gamma_{1,2}$ is 1.1 cm^{-1} , which is in the range between the L (0 cm^{-1}) and ZR (1.7 cm^{-1}) values. This is in reasonable agreement with the anisotropy of mercury iodide, which should differentiate acoustic-phonon branches with different polarizations.²⁰ In addition, the $2\Gamma_{1,2}$ values vary from 1.1 cm^{-1} at room

temperature to 0.6 cm^{-1} at 150 K and, within the experimental error, a linear behavior with the temperature is displayed. Since many-body theory yields a displacement proportional to T for all the $G_{i,j}$ elements [Eq. (8)], as far as the coupling is due to cubic anharmonicity, further confidence can be placed in this approach.

IV. FINAL MARKS

We have studied anharmonic mixing between low-energy modes in mercury iodide. Previous experimental and theoretical investigations showed the existence of the two limiting situations characterized, respectively, by no phonon mixing or by a strong interference effect.⁵ In this work new experimental evidence on the intermediate situation is reported for HgI_2 . We have shown that the finite lifetime of E_g low-frequency vibrations is principally due to anharmonic interaction. A new model based on the many-body formalism has also been developed in order to reproduce experimental spectra. The agreement between theory and experimental results has been found to be quite satisfactory for all temperatures we have studied. Finally, we have also discussed in detail the physical meaning of the $G_{i,j}$ parameters in relation to the microscopic dynamics of anharmonic processes.

*Present address: Institut de Physique Appliquée, Ecole Polytechnique Fédérale de Lausanne, CH-1015 Lausanne, Switzerland.

¹J. F. Scott, *Rev. Mod. Phys.* **46**, 86 (1974); J. F. Scott, *Phys. Rev. Lett.* **24**, 1107 (1970).

²D. L. Rousseau and S. P. S. Porto, *Phys. Rev. Lett.* **20**, 1354 (1968).

³V. M. Agranovich and I. I. Lalov, *Usp. Fiz. Nauk* **146**, 267 (1985) [*Sov. Phys.—Usp.* **28**, 484 (1985)].

⁴U. Fano, *Phys. Rev.* **124**, 1866 (1961).

⁵A. Zawadowski and J. Ruvalds, *Phys. Rev. Lett.* **24**, 1111 (1970).

⁶R. F. Wallis, I. P. Ipatova, and A. A. Maradudin, *Fiz. Tverd. Tela (Leningrad)* **8**, 1064 (1966) [*Sov. Phys.—Solid State* **8**, 850 (1966)].

⁷V. A. Haisler, V. M. Zaletin, and A. F. Kravchenko, *Phys. Status Solidi B* **125**, K103 (1984).

⁸V. A. Haisler, V. M. Zaletin, A. F. Kravchenko, and G. Y. Yashin, *Phys. Status Solidi B* **121**, K13 (1984).

⁹N. Kuroda, M. Sakai, and Y. Nishina, *J. Phys. Soc. Jpn.* **54**, 1423 (1985).

¹⁰N. Kuroda, T. Iwabuchi, and Y. Nishina, *J. Phys. Soc. Jpn.*

52, 2419 (1983).

¹¹A. Anedda, G. Bongiovanni, and E. Fortin, *Phys. Status Solidi B* **146**, 757 (1988).

¹²S. Nakashima and M. Balkansky, *Phys. Rev. B* **34**, 5801 (1986).

¹³A. Anedda and G. Bongiovanni (unpublished).

¹⁴A. A. Abrikosov, L. P. Gor'kov, and I. E. Dzyaloshinskii, in *Methods of Quantum Field Theory in Statistical Physics*, edited by R. Silverman (Prentice-Hall, Englewood Cliffs, NJ, 1963).

¹⁵A. A. Maradudin and A. E. Fein, *Phys. Rev.* **128**, 2589 (1962).

¹⁶I. P. Ipatova, A. A. Maradudin, and R. F. Wallis, *Phys. Rev.* **155**, 882 (1967).

¹⁷M. Born and K. Huang, in *Dynamical Theory of Crystal Lattices* (Oxford University Press, New York, 1954).

¹⁸The expression of ω_0 is different from the one given by ZR. This is due to the approximation form of the phonon propagator they consider.

¹⁹T. Sakurai and T. Sato, *Phys. Rev. B* **4**, 583 (1971).

²⁰B. Prevot, C. Schwab, and B. Dorner, *Phys. Status Solidi B* **88**, 327 (1978).